Artifact Reduction in Radiometric Compensation of Projector-Camera Systems for Steep Reflectance Variations

Shoichiro Mihara, Daisuke Iwai, and Kosuke Sato, *Member, IEEE*

***Abstract*—In this paper, we propose a novel radiometric compensation method that applies a high-spatial-resolution camera to a projector-camera system to reduce the artifacts around the regions where the reflectance of the projection surface changes steeply. The proposed method measures the reflection in the region of a single projector pixel on a projection surface with multiple camera pixels. From the measurement, it computes multiple color-mixing matrices, each of which represents a color space conversion between each camera and the projector pixels. Using these matrices, we calculate the optimal projection color by applying the linear least squares method, so that the displayed color in the projector pixel region is as close as possible to the target appearance. Through projection experiments, we confirm that our proposed method reduces the artifacts around the regions where the reflectance changes steeply, when compared with other conventional compensation methods.**

***Index Terms*—High-resolution camera, projector-camera systems (ProCams), radiometric compensation, steep reflectance variation.**

I. Introduction

When an image is projected onto an everyday surface rather than a normal projection screen from a video projector, the displayed results are visually disturbed due to the mixture of the projected color with the surface texture. This leads to image quality degradation of the projected appearance. To solve this problem, researchers working in the field of projector-camera systems (ProCams) have been working on radiometric compensation techniques [1]. These techniques modify the colors of a projection image to display the desired appearance on a textured surface. To achieve this goal, the techniques measure the spatially varying reflectance of the surface using a color camera. Potential applications include an interactive system of projection-based augmented reality (AR) [2], home theater in a room where a textured wall or curtain is used as a projection screen [3], projection-based restoration of pictorial art or historically important objects with faded colors [4], [5], and projection-based art installation (known as projection mapping) that projects images onto a large building.

Manuscript received May 31, 2013; revised December 18, 2013 and January 30, 2014; accepted February 28, 2014. Date of publication March 5, 2014; date of current version August 31, 2014. This work was supported by a Grant-in-Aid for Scientific Research on Innovative Areas Shitsukan under Grant 22135003 through the Ministry of Education, Culture, Sports, Science, and Technology, Japan. This paper was recommended by Associate Editor A. Kaup.

The authors are with the Graduate School of Engineering Science, Osaka University, Toyonaka, Osaka 560-8531, Japan (e-mail: daisuke.iwai@sys.es.osaka-u.ac.jp).

Color versions of one or more of the figures in this paper are available online at http://ieeexplore.ieee.org.

Digital Object Identifier 10.1109/TCSVT.2014.2309832

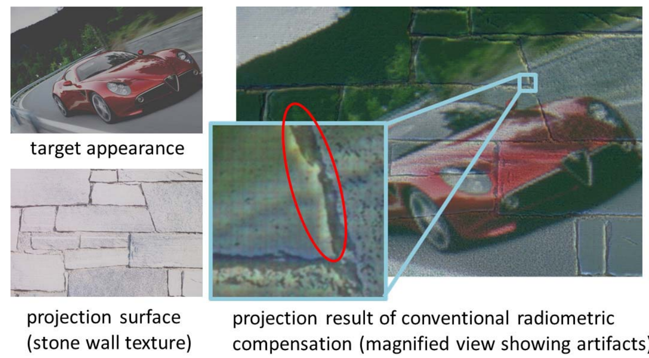

Fig. 1. Artifacts occur around the edges of the stone wall texture when conventional radiometric compensation is applied. The red ellipse indicates an unnaturally bright region.

A technical issue of radiometric compensation is the lack of color reproduction accuracy due to the low spatial resolution of the projector. A projected pixel illuminates a certain region on a projection surface rather than an infinitesimal point. In addition, the reflectance in that region is not uniform for most of the ordinary surfaces. Therefore, we cannot perfectly compensate for the projected result, and artifacts occur because the reflection within the region varies spatially. The artifacts become significant when the reflectance steeply varies within the region, such as on the edge of a surface texture. Observers will notice the artifacts when their viewpoints are so close to the projection surface as they can see individual projected pixels. Such a situation can frequently occur, for example, in a projection-based AR application where a user touches or holds a projected object and in a museum where a visitor sees a historically important object, whose color is restored by projected imagery, up close. Fig. 1 shows an example of artifacts that occur around the edges of a stone wall texture. In this example, we can confirm that the reflected colors around the edges become unnaturally bright.

This paper aims to minimize the artifacts of radiometric compensation in each projected pixel region where the reflectance of the projection surface steeply varies in the spatial domain. To achieve this goal, we propose to use an off-the-shelf high-spatial-resolution camera that can capture images with a resolution greater than 10 mega pixels to densely measure spatially varying reflectance in a projected pixel region on the surface. Based on this measurement, we compute the

1051-8215 © 2014 IEEE. Personal use is permitted, but republication/redistribution requires IEEE permission.
See http://www.ieee.org/publications_standards/publications/rights/index.html for more information.

Authorized licensed use limited to: Tsinghua University. Downloaded on October 10,2022 at 07:45:50 UTC from IEEE Xplore. Restrictions apply.

projection color that minimizes the color difference between the target and the displayed appearance in the pixel region in the usual least squares manner. This paper explains the proposed principle and shows how the proposed technique improves compensation accuracy by conducting a projection experiment in which we compared the results of the proposed technique with those of conventional technique.

II. Related Work

The purpose of radiometric compensation is to make the projected result as close as possible to the desired appearance [1]. The core of the radiometric compensation technique is to calibrate the color space conversion between the input color of the projector pixel and the reflected color on the projection surface captured by the corresponding camera pixel. Note that, in general, the radiometric compensation technique regards the ProCams camera as the eye of an observer. Once the calibration is done, one can compute the optimal input color to a projector pixel and display the desired appearance on the surface by projecting the computed colors, as long as they are within the projector's color gamut.

Prior to the calibration, pixel correspondences between the projector and the camera need to be obtained. Previous studies applied the gray-code pattern projection technique [6], which is well known for 3-D shape measurement in the computer vision research field. We also apply this technique to our research to obtain pixel correspondences. Although previous studies assume that one projector pixel corresponds to one camera pixel (one-to-one mapping), in this paper we assume that a single projector pixel region is measured by multiple camera pixels (one-to-many mapping).

Bimber *et al.* [3] proposed a simple color space conversion model by assuming that each color channel of a camera pixel is affected only by the same color channel of the corresponding projector pixel. Nayar *et al.* [7] proposed a more complex model that considers the color-mixing effect resulting from the difference between the broadband spectral property of an RGB color filter attached to a camera pixel and that attached to the corresponding projector pixel. For example, even if we input a pure red color to a projector pixel and capture the projected result by the corresponding camera pixel, the green and blue responses of the camera pixel do not become zero. Nayar *et al.* introduced a 3×3 color-mixing matrix to solve this problem. Yoshida *et al.* [4] proposed a different color-mixing matrix, which accounts for the environmental light and the projector's black offset. Even if the projector projects a uniform black image, the projection area is brightened by the projector's black offset and the environmental lights. Therefore, the accuracy of radiometric compensation of Yoshida's method is theoretically higher than that of other approaches described above. However, one cannot perfectly compensate for a projected result, especially on a low reflectance (i.e., black) surface, due to the limited color gamut (including dynamic range) of current off-the-shelf projectors. Some researchers solved this problem by adjusting the intensity or colors of target appearances [8], [9]. These approaches adapt the image content (sometimes based on the capabilities of the human visual system) to reduce artifacts.

None of the previous approaches have explicitly focused on visual artifacts resulting from the spatially varying reflectance within a single projected pixel region. The purpose of this paper is to minimize artifacts and consequently improve the compensated image quality based on a dense calibration of the color space conversions within a single projected pixel region using a high-spatial-resolution camera.

III. Radiometric Compensation Using a High-Resolution Camera

In this paper, we use a high-resolution camera to capture an image with a resolution greater than 10 mega pixels, to densely calibrate color space conversions within a single projected pixel region. First, this section briefly describes Yoshida's radiometric compensation technique [4], which is the conventional approach and the base of our proposed technique. Second, it describes the proposed principle. Third, we compare the conventional and proposed techniques, and explain why the proposed technique can theoretically provide better projection results than the conventional one.

In this paper, we assume that the reflectance property of a projection surface is Lambertian. We measure pixel correspondences between the camera and the projector in our ProCams using the gray-code pattern projection technique [6].

A. Conventional Technique

Yoshida *et al.* proposed to model the color space conversion from an input color (R_P, G_P, B_P) for a projector pixel to the captured color (R_C, G_C, B_C) of the corresponding camera pixel using the following linear equation:

$$\boldsymbol{C} = \boldsymbol{K}\boldsymbol{P} \tag{1}$$

where $\boldsymbol{C} = [R_C\ G_C\ B_C\ 1]^t$, $\boldsymbol{P} = [R_P\ G_P\ B_P\ 1]^t$ and

$$\boldsymbol{K} = \begin{bmatrix} k_{11} & k_{12} & k_{13} & k_{14} \\ k_{21} & k_{22} & k_{23} & k_{24} \\ k_{31} & k_{32} & k_{33} & k_{34} \\ 0 & 0 & 0 & 1 \end{bmatrix}. \tag{2}$$

Here, $\boldsymbol{K}$ is a color-mixing matrix containing the spectral characteristics of the projector and camera, the reflectance of the surface, environmental light, and form factors such as the distance of the projector/camera from the surface and the incident angle of the projected light. Once $\boldsymbol{K}$ is calibrated, we can estimate the captured color value (R_C, G_C, B_C) when (R_P, G_P, B_P) is sent to the corresponding projector pixel using (1). Inversely, we can also compute the color value (R_P, G_P, B_P) that should be sent to the projector pixel to display a desired appearance (R_C, G_C, B_C) using

$$\boldsymbol{P} = \boldsymbol{K}^{-1}\boldsymbol{C}. \tag{3}$$

Here, $\boldsymbol{K}$ contains 12 unknown elements $k_{11}, \ldots, k_{34}$. Suppose, we project a color from the projector and capture the displayed pixel with the camera. The pair of input and captured colors provides us with three equations relating to the matrix elements, which are decomposed from (1). Therefore, we can solve the elements once we have at least four pairs that provide us with 12 equations. With more than four pairs, we

Authorized licensed use limited to: Tsinghua University. Downloaded on October 10,2022 at 07:45:50 UTC from IEEE Xplore. Restrictions apply.

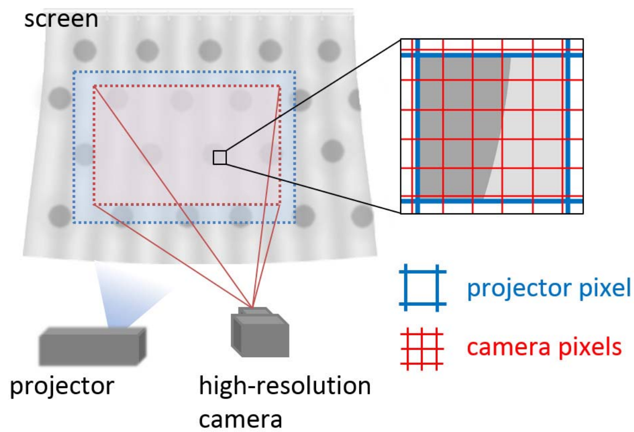

Fig. 2. Pixel correspondences between a projector and a high-resolution camera.

can solve them more accurately using the usual least squares method.

Yoshida's approach calibrates $\boldsymbol{K}$ for each projector pixel by assuming that the projector pixel corresponds to only a single camera pixel and that the reflectance within the projector pixel region is uniform. Therefore, a visual artifact (i.e., the error between a target appearance and the projected result) occurs when the reflectance within a projected pixel region spatially varies.

B. Proposed Technique

Explicitly considering the spatially varying reflectance within a projected pixel region, we propose a radiometric compensation technique that uses a high-spatial-resolution camera to measure the region with multiple camera pixels, as shown in Fig. 2. The proposed technique calibrates the color-mixing matrix $\boldsymbol{K}$ for each camera pixel. Therefore, multiple $\boldsymbol{K}$s are computed for each projector pixel.

Multiple input colors can be computed for a single projector pixel using (3). However, it is impossible to simultaneously project the computed multiple color values from the pixel. Therefore, the open question here is how should the input color value for a projector pixel be determined from multiple color-mixing matrices of the corresponding camera pixels? Our solution determines the input color value so as to minimize the color differences between the target and the displayed appearances.

Let N be camera pixels measuring the same projector pixel. The color-mixing matrix $\boldsymbol{K_i}$ $(i = 1, \ldots, N)$ for each camera pixel i is calibrated in the same manner, as the conventional technique explained in Section III-A. We denote the elements of each matrix $\boldsymbol{K_i}$ as $k^i_{11}, \ldots, k^i_{34}$. When an input color value $\boldsymbol{P}$ is sent to a projector pixel, the camera pixels corresponding to that projector pixel observe different reflected colors $\boldsymbol{C_i} = [R^i_C \; G^i_C \; B^i_C \; 1]^t$ $(i = 1, \ldots, N)$. Based on (1), the relationship between $\boldsymbol{P}$ and $\boldsymbol{C_i}$ can be represented using $\boldsymbol{K_i}$ as

$$\boldsymbol{C_i} = \boldsymbol{K_i}\boldsymbol{P}. \tag{4}$$

Let $\boldsymbol{T} = [R_T \; G_T \; B_T \; 1]^t$ be the target appearance of the projector pixel region. We define our error metric e as the sum of square errors between the target color $\boldsymbol{T}$ and each reflected color $\boldsymbol{C_i}$ over the projector pixel region

$$e = \sum_{i=1}^{N} \|\boldsymbol{T} - \boldsymbol{C_i}\|_2 = \sum_{i=1}^{N} \|\boldsymbol{T} - \boldsymbol{K_i}\boldsymbol{P}\|_2. \tag{5}$$

The reflected color of the projector pixel region is closest to the target appearance when a projection color $\boldsymbol{P^*}$ that minimizes the error metric e is projected

$$\boldsymbol{P^*} = \arg\min_{\boldsymbol{P}} e. \tag{6}$$

We can solve this problem using the least squares method. Suppose, vector $\boldsymbol{T_s}$ and matrix $\boldsymbol{K_s}$ are obtained by stacking the vector $\boldsymbol{T}$ and matrix $\boldsymbol{K_i}$, respectively, as

$$\boldsymbol{T_s} = \begin{bmatrix} \boldsymbol{T} \\ \vdots \\ \boldsymbol{T} \end{bmatrix}, \quad \boldsymbol{K_s} = \begin{bmatrix} \boldsymbol{K_1} \\ \vdots \\ \boldsymbol{K_N} \end{bmatrix}. \tag{7}$$

Then, the optimal projection color $\boldsymbol{P^*}$ can be computed using the linear least squares method as

$$\boldsymbol{P^*} = (\boldsymbol{K_s^t}\boldsymbol{K_s})^{-1}\boldsymbol{K_s^t}\boldsymbol{T_s}. \tag{8}$$

C. Theoretical Comparison

In this section, we show the theoretical advantage of our proposed technique over the conventional one [4]. According to the definition of the least squares method, it is theoretically true that the proposed technique provides the optimum input color $\boldsymbol{P^*}$ that minimizes the error e of (5). In the following part of this section, it will be shown that the conventional technique provides an input color that is different from the optimum one.

The conventional radiometric compensation (1) can be regarded as an error minimization problem as

$$\boldsymbol{P^*_{\mathbf{conv}}} = \arg\min_{\boldsymbol{P}} \|\boldsymbol{T} - \boldsymbol{K}\boldsymbol{P}\|_2. \tag{9}$$

This minimization problem can be reformulated as

$$\boldsymbol{P^*_{\mathbf{conv}}} = \arg\min_{\boldsymbol{P}} \sum_{i=1}^{N} \|\boldsymbol{T} - \boldsymbol{K}\boldsymbol{P}\|_2. \tag{10}$$

Comparing (5) and (6) with (10), we can confirm that $\boldsymbol{P^*}$ and $\boldsymbol{P^*_{\mathbf{conv}}}$ take different values except when $i = 1$ or $\boldsymbol{K_i} = \boldsymbol{K_j}, (\forall j \neq i)$. The former condition holds when a projector pixel corresponds to a single camera pixel (one-to-one mapping), and the latter holds when the reflectance in a projector pixel region is uniform. In other words, an input color computed by the conventional technique is different from the one computed by the proposed technique, except when the assumption of the conventional technique holds. Therefore, the proposed technique provides a better projection result than the conventional one.

IV. Evaluation

We conducted a projection experiment to evaluate the proposed method by comparing its projection results with the methods of [4] and [7]. First, we explain about our

Authorized licensed use limited to: Tsinghua University. Downloaded on October 10,2022 at 07:45:50 UTC from IEEE Xplore. Restrictions apply.

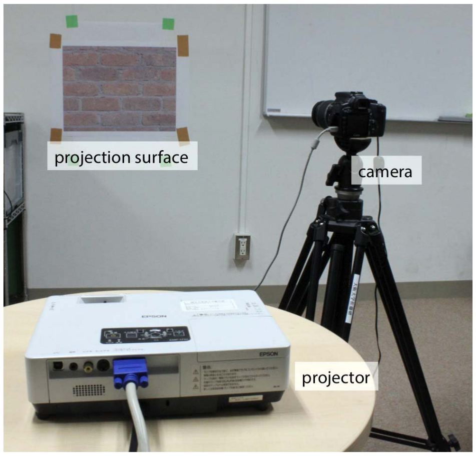

Fig. 3. Experimental system.

(a) (b) (c)

Fig. 4. Projection surfaces under environment light captured by the camera of the experimental system. (a) Color pattern printed paper (COLOR PAPER). (b) Brick pattern printed paper (BRICK PAPER). (c) Textured cloth (CLOTH).

experimental system and calibration process. Then, we show the projection results and compare the image qualities of different radiometric compensation methods.

A. Experimental System and Calibration

We conducted our experiments with a high-spatial-resolution camera (Canon EOS Kiss Digital X, 10.1 mega pixels) and two projectors: a three-LCD projector (EPSON EMP-1710, 2700 lm, 800×600 pixels) and a single chip digital light processing (DLP) projector (NEC NP110, 2200 lm, 800×600 pixels). The distances from the projector and camera to the projection surface were 2.0 and 1.3 m, respectively (Fig. 3). We used a part of a captured camera image in the experiments, which was a rectangular area of 800×600 pixels. In the experimental system, each projected pixel was captured by 64 ($= 8 \times 8$) camera pixels on average (i.e., $N = 64$). Therefore, an area of projection of 100×75 pixels was used in the experiment. In the rest of this paper, this area is referred to as the working area.

We prepared three different types of projection surfaces:

1) a piece of paper with a printed color pattern (COLOR PAPER);
2) a piece of paper with a printed brick pattern (BRICK PAPER);
3) a textured cloth (CLOTH).

The pieces of paper were glued to a wall to make them flat, while the cloth was hung without being flattened. Fig. 4 shows the cropped version of the projection surfaces that were captured by the camera, corresponding to the working areas.

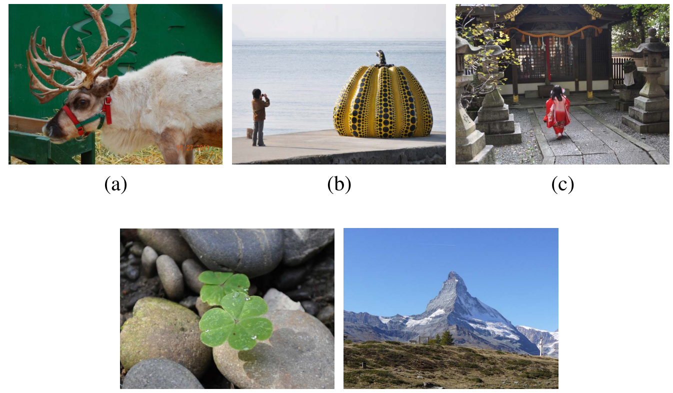

(a) (b) (c)

(d) (e)

Fig. 5. Target images. (a) Animal. (b) Pumpkin. (c) Girl. (d) Stone. (e) Mountain.

The gray-code pattern projection technique was performed to acquire pixel correspondences between the camera and the projector on the surfaces. Then, color-mixing matrices were calibrated by projecting 29 uniform colors including black. In the proposed method, the calibration was performed for each camera-to-projector pixel correspondence. Because multiple camera pixels shared a single projector pixel, multiple color-mixing matrices were computed for a projector pixel. In the conventional methods, the calibration was performed for each correspondence between a projector pixel and a virtual camera pixel. We regarded multiple camera pixels that shared the same projector pixel as a virtual low-resolution camera pixel. The color value of the virtual pixel was computed by averaging the values of the corresponding camera pixels. Then, in the conventional methods, a single matrix was calibrated for each projector pixel in contrast to the proposed method.

The gray-code pattern projection and color-mixing matrix calibration were performed every time an element of the system (either projector or surface) was changed.

B. Projection Experiment

We conducted projection experiments using the LCD and DLP projectors and projection surfaces shown above. We paired one of the projectors with one of the surfaces in three ways: 1) LCD projector and COLOR PAPER; 2) DLP projector and BRICK PAPER; and 3) DLP projector and CLOTH. Five target images (Fig. 5) were set for each pair. We computed four types of projection images for each target image. One of the projection images was the target image itself, and the others were computed using the compensation methods. Therefore, we conducted 60 experiments ($= 3$ pairs $\times$ 5 target images $\times$ 4 methods).

Figs. 6–8 show the examples of modified target images and the projection results of all the compensation methods, as well as those without compensation under three different conditions. The target images were modified so that the spatial resolution was downsampled according to the number of projector pixels in the working area. The projection results were captured by the camera of the system, which was used in the calibration of the radiometric compensation.

Authorized licensed use limited to: Tsinghua University. Downloaded on October 10,2022 at 07:45:50 UTC from IEEE Xplore. Restrictions apply.

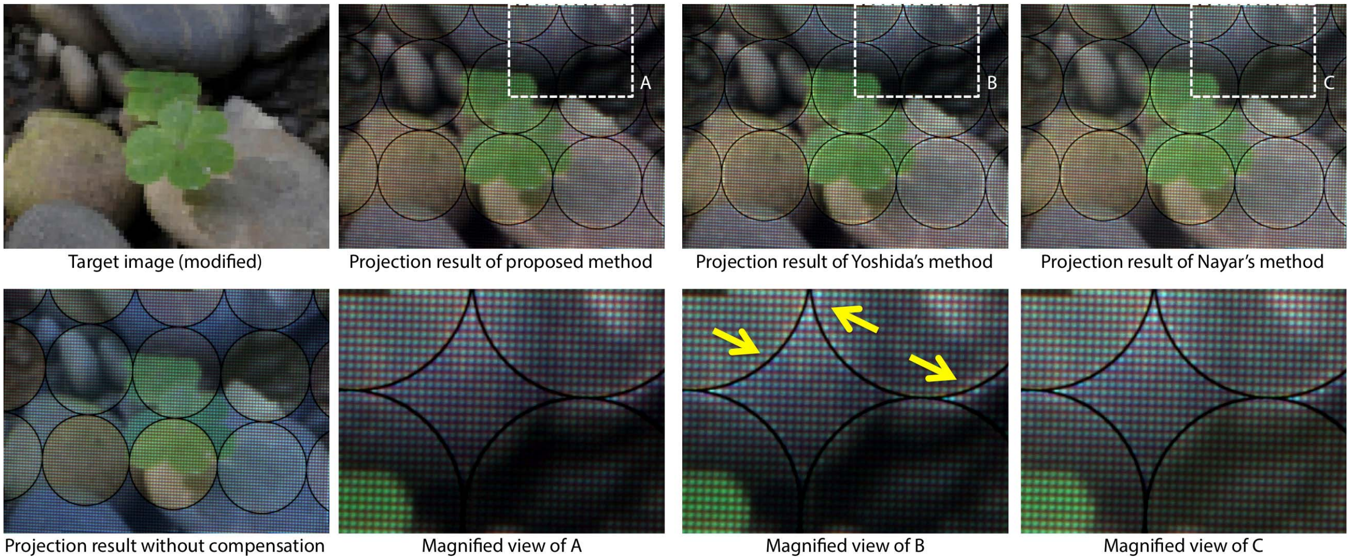

Fig. 6. Projection results (projector: LCD, surface: COLOR PAPER, and target image: stone). Yellow arrows: unnaturally bright areas.

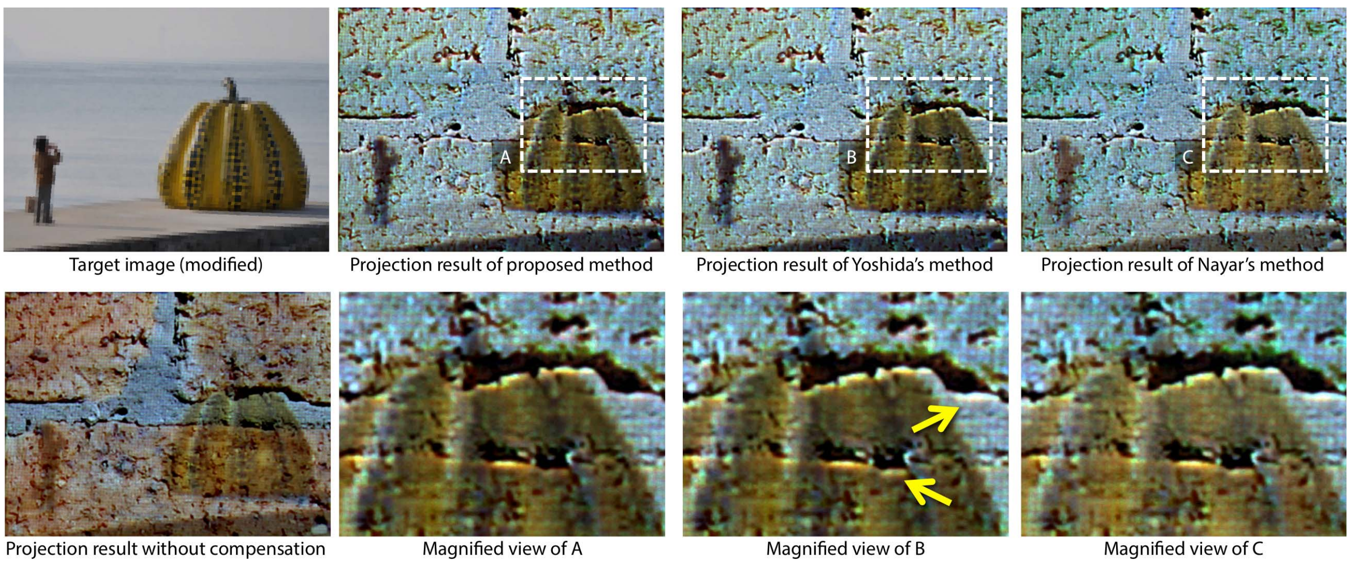

Fig. 7. Projection results (projector: DLP, surface: BRICK PAPER, and target image: pumpkin). Yellow arrows: unnaturally bright areas.

One could clearly see improvements in the results of the proposed method compared with those of the other methods. Specifically, the proposed method reproduces the target images the most closely. Yoshida's method provides results that have unnaturally brighter areas around the edges of surface textures. Nayar's method provides results the farthest from the target images with perceivable contrast compression and bright areas around edges. Fig. 9 shows the color differences between the target appearance and projected results.

To compare the results quantitatively, we compute Delta E (the Euclidean distance in CIELAB color space) on a per-pixel basis between the modified target image and each projection result. Fig. 10 shows an example of the Delta E map as a grayscale representation. We also calculated the average of the Delta E over the full image area, which is shown in Table I. As can be observed, besides the perceived improvements shown in Figs. 6–8, the proposed method provides projection results with less Delta E than the other methods in all the cases. Especially, the proposed technique provides superior results to those of the conventional methods around areas where reflectances steeply vary.

V. Discussion

From the experimental results, we confirmed that our method generally has the best image reproducibility. This section discusses the reasons behind these results and the limitations of our method.

Nayar's method provided results with the largest amount of errors in all the cases, because it does not consider the environment light and the black offset of a projector. Since such offsets exist in the experimental environment (and also in usual usage scenarios), Nayar's method over- or under-estimate the optimal projection image.

Yoshida's method provided better results than Nayar's method. Although it provided comparable results with our

Authorized licensed use limited to: Tsinghua University. Downloaded on October 10,2022 at 07:45:50 UTC from IEEE Xplore. Restrictions apply.

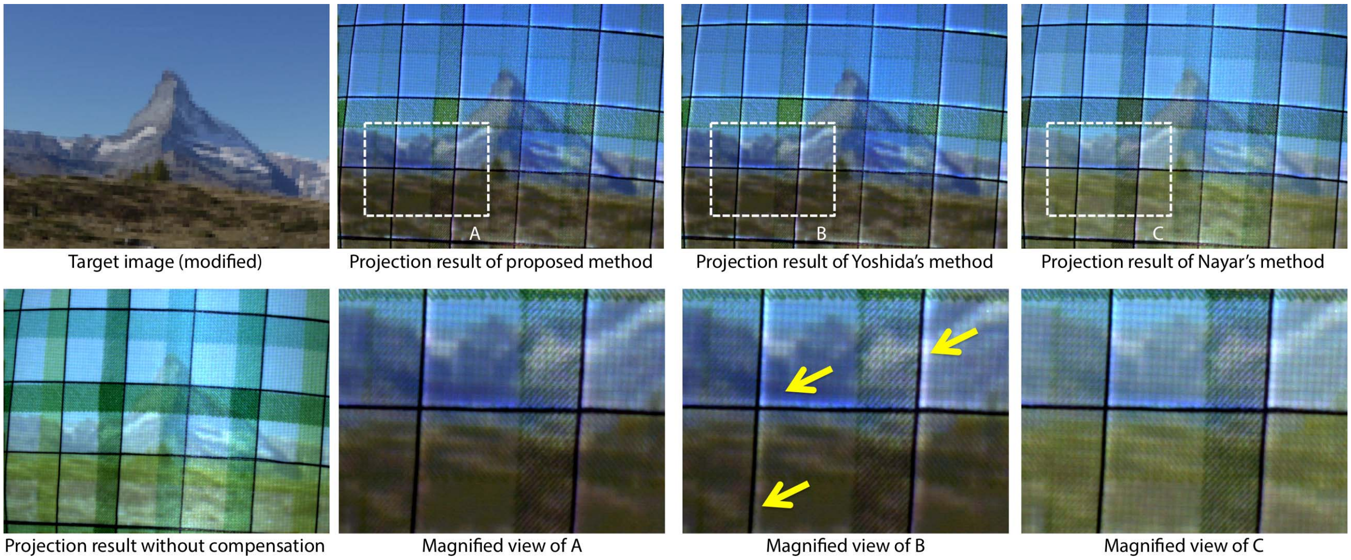

Fig. 8. Projection results (projector: DLP, surface: CLOTH, and target image: mountain). Yellow arrows: unnaturally bright areas.

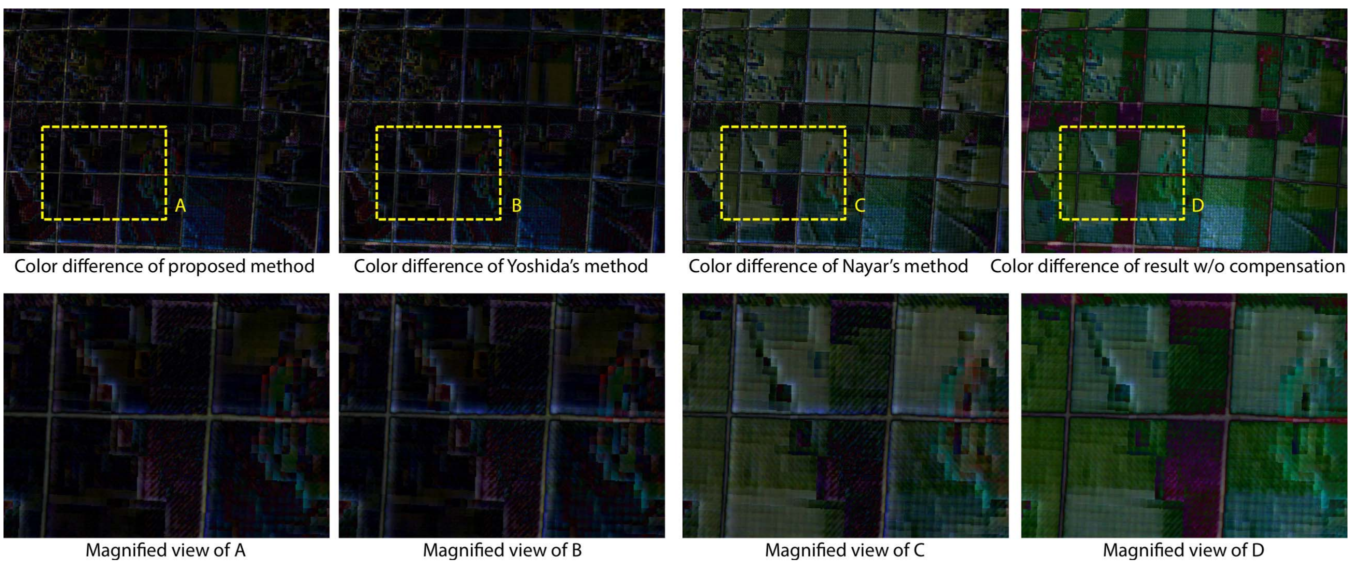

Fig. 9. Color difference visualization (projector: DLP, surface: CLOTH, and target image: girl).

method in most part of the images, unnaturally bright spots resulted at around the edges of the surface textures. A very dark pigment such as black ink in a projector pixel area significantly decreases the averaged reflectance of the area. In such a case, Yoshida's method computes the input color with unnecessarily high intensity to compensate for the area with low average-reflectance, resulting in undesirably bright spots in areas other than the dark-pigment pixel area.

From a different point of view, the major gain in the proposed method is caused by the method for measuring the error. Suppose that one projector pixel covers a surface region, and black and white pigments split the region. The conventional methods (Nayar and Yoshida) calculate the error as the difference from the average color of the region to the target. In this case, the brightness of the projection result in the white pigment area is always brighter than the target to compensate for the black pigment area, i.e., to make the average brightness of the whole region close to the target. On the other hand, the proposed method calculates the error on a finer grid. In this case, the error in the black pigment area less affects the projection result in the white pigment area than the conventional methods. In other words, the projection color is calculated so that the projection result in the white pigment area is close to the target color for making the error smallest. Therefore, a distant viewer who sees the average brightness might prefer the conventional methods. On the other hand, for a close viewer who sees subpixels, the proposed method would look better.

Our method shares some limitations with other radiometric compensation methods. First, it only supports surfaces having Lambertian reflectance, and it does not work for those having specular reflectance. Second, our method cannot deal with

Authorized licensed use limited to: Tsinghua University. Downloaded on October 10,2022 at 07:45:50 UTC from IEEE Xplore. Restrictions apply.

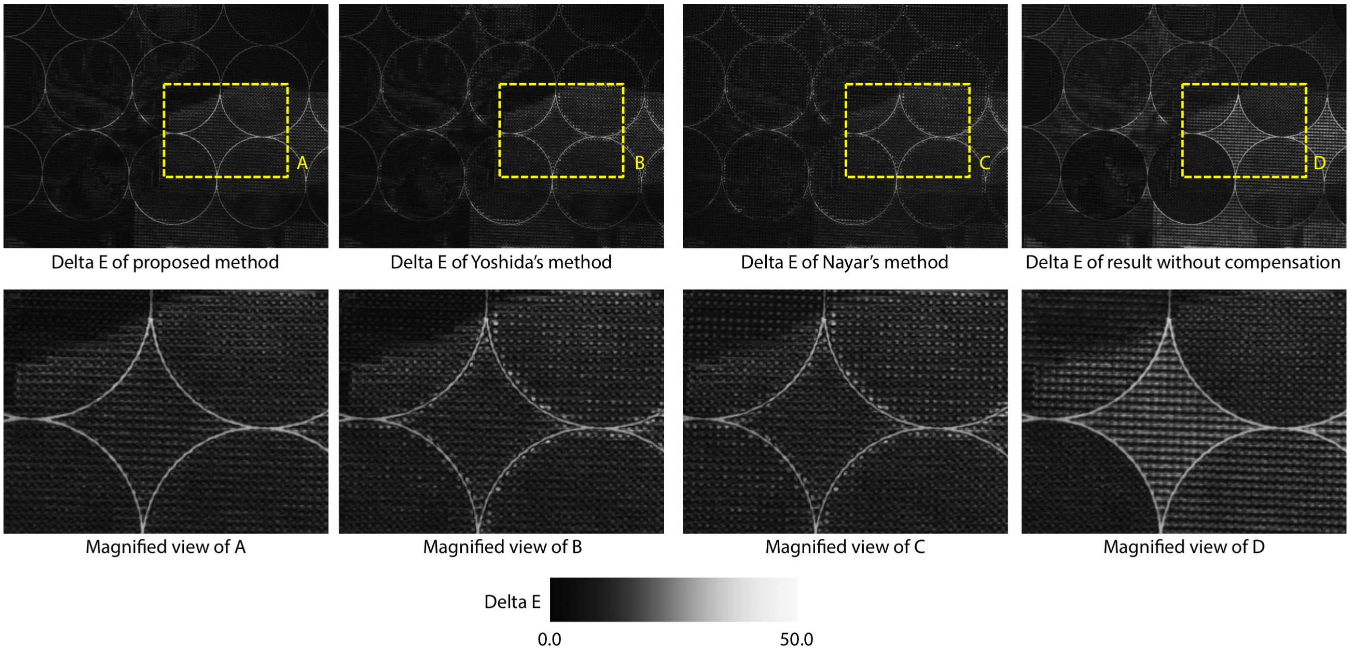

Fig. 10. Delta E visualization (projector: LCD, surface: COLOR PAPER, and target image: animal).

TABLE I

DELTA E EVALUATION RESULTS. BOLD NUMBERS INDICATE THE MINIMUM AMONG FOUR METHODS

		animal	pumpkin	girl	stone	mountain
LCD/ COLOR PAPER	proposed	**8.17**	**10.02**	**7.73**	**8.01**	**9.22**
	Yoshida	8.20	10.09	7.75	8.03	9.35
	Nayar	9.22	10.52	8.85	9.13	9.75
	w/o compensation	11.37	12.87	10.10	10.74	11.12
DLP/ BRICK PAPER	proposed	**11.04**	**9.78**	**8.52**	**8.57**	**9.31**
	Yoshida	11.19	10.07	9.00	9.04	9.80
	Nayar	11.44	11.15	10.10	9.90	10.06
	w/o compensation	13.43	12.71	11.61	11.81	12.34
DLP/ CLOTH	proposed	**8.72**	**7.68**	**6.77**	**7.40**	**7.37**
	Yoshida	8.76	7.81	6.99	7.58	7.61
	Nayar	12.31	9.51	12.20	11.43	10.22
	w/o compensation	16.46	16.43	17.64	16.80	16.28

global lighting effects such as interreflection and subsurface scattering. Although, we can theoretically solve these problems by analyzing light transport information between the projector and camera on the surface, the computational cost greatly increases so that it is intractable to solve in a reasonable computational time. The Delta E values are relatively low in all the cases, and there are still many visible artifacts in the compensated results. The main reason for the image quality degradation is that the dynamic range of the target color exceeds the limited color gamut of the system. Therefore, clipping errors occurred, which resulted in the high Delta E values.

VI. CONCLUSION

We proposed and implemented a novel radiometric compensation method that applied a 10 mega pixel camera to a ProCams to reduce the artifacts around the edges where the reflectance of the projection surface changed steeply. The proposed method measured the reflection of a single projected pixel region on a projection surface with multiple camera pixels, and then computed multiple color-mixing matrices for the projected pixel. Using these matrices, we calculated the optimal projection color by applying the linear least squares method so that the displayed colors in the projector pixel region were as close as possible to the target appearance. Through projection experiments with LCD and DLP projectors and three different projection surfaces, we confirmed that the proposed method improved the compensation accuracy (evaluated with Delta E), as compared with the conventional methods. In the future work, we will attempt to speed up the process using parallel processing on a graphics processing unit.

REFERENCES

[1] O. Bimber, D. Iwai, G. Wetzstein, and A. Grundhöfer, "The visual computing of projector-camera systems," *Comput. Graph. Forum*, vol. 27, no. 8, pp. 2219–2254, 2008.

[2] O. Bimber and R. Raskar, *Spatial Augmented Reality: Merging Real and Virtual Worlds*. Natick, MA, USA: A. K. Peters Ltd., 2005.

[3] O. Bimber, A. Emmerling, and T. Klemmer, "Embedded entertainment with smart projectors," *IEEE Comput.*, vol. 38, no. 1, pp. 56–63, Jan. 2005.

[4] T. Yoshida, C. Horii, and K. Sato, "A virtual color reconstruction system for real heritage with light projection," in *Proc. Int. Conf. Virtual Syst. Multimedia*, 2003, pp. 161–168.

Authorized licensed use limited to: Tsinghua University. Downloaded on October 10,2022 at 07:45:50 UTC from IEEE Xplore. Restrictions apply.

[5] D. G. Aliaga, A. J. Law, and Y. H. Yeung, “A virtual restoration stage for real-world objects,” *ACM Trans. Graph.*, vol. 27, no. 5, pp. 149:1–149:10, 2008.

[6] K. Sato and S. Inokuchi, “Range-imaging system utilizing nematic liquid crystal mask,” in *Proc. IEEE Int. Conf. Comput. Vis.*, 1987, pp. 657–661.

[7] S. K. Nayar, H. Peri, M. D. Grossberg, and P. N. Belhumeur, “A projection system with radiometric compensation for screen imperfections,” in *Proc. IEEE Workshop Projector-Camera Syst.*, 2003.

[8] M. Ashdown, T. Okabe, I. Sato, and Y. Sato, “Robust content-dependent photometric projector compensation,” in *Proc. IEEE Workshop Projector-Camera Syst.*, 2006.

[9] A. Grundhöfer and O. Bimber, “Real-time adaptive radiometric compensation,” *IEEE Trans. Visualizat. Comput. Graph.*, vol. 14, no. 1, pp. 97–108, Feb. 2008.

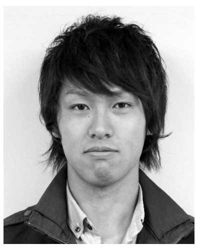

Shoichiro Mihara received the B.S. and M.S. degrees from Osaka University, Suita, Japan, in 2012 and 2014, respectively.

He is with KDDI Corporation, Tokyo, Japan. His research interests include projection-based mixed reality and projector-camera systems.

Daisuke Iwai received the B.S., M.S., and Ph.D. degrees from Osaka University, Suita, Japan, in 2003, 2005, and 2007, respectively.

He was a Visiting Scientist with Bauhaus University Weimar, Weimar, Germany, from 2007 to 2008, and a Visiting Associate Professor with ETH Zurich, Zurich, Switzerland, in 2011. He is currently an Associate Professor with the Graduate School of Engineering Science, Osaka University. His research interests include human–computer interaction and projection-based mixed reality.

Kosuke Sato (M’14) received the B.S., M.S., and Ph.D. degrees from Osaka University, Suita, Japan, in 1983, 1985, and 1988, respectively.

He was a Visiting Scientist with the Robotics Institute, Carnegie Mellon University, Pittsburgh, PA, USA, from 1988 to 1990. He is currently a Vice Dean with the Graduate School of Engineering Science, Osaka University. His research interests include image sensing, 3-D image processing, digital archiving, and virtual reality.

Dr. Sato is a member of the Association for Computing Machinery.

Authorized licensed use limited to: Tsinghua University. Downloaded on October 10,2022 at 07:45:50 UTC from IEEE Xplore. Restrictions apply.